ELECTRO-HYDROSTATIC COMPACT DRIVES WITH VARIABLE TRANSMISSION RATIO

Giacomo Kolks*, Jürgen Weber

Institut of Mechatronic Engineering, Technische Universität Dresden, Helmholtzstrasse 7a, 01069 Dresden
* Corresponding author: Tel.: +49 351 46339932; E-mail address: giacomo.kolks@tu-dresden.de

ABSTRACT

Electro-hydrostatic compact drives are an emerging technology within a range of industrially available translational drive solutions, combining the specific advantages of hydraulic and electromechanical screw drives. Compared to electromechanical screw drives, hydrostatic drives can vary their transmission ratio with comparably little effort, giving them the key advantage of downsizing the electric drive components for a given load cycle.

This paper provides a guideline on how to calculate the downsizing potential of electric motors and inverters arising from variable transmission ratio based on the load regime of a given application. Furthermore, a comprehensive systematisation of the actual switching process is described for systems that are switched by means of switching valves. The presented set of methodology is applied to demonstrators in order to validate the general findings.

Keywords: electro-hydrostatic compact drive, variable transmission, switching hydraulics

1. INTRODUCTION

Machine manufacturers are increasingly in demand of modular and self-contained drive solutions with high energy efficiency – without abandoning the traditional benefits of hydraulic cylinder drives, such as robustness and high force density. Electro-hydrostatic compact drives (ECD) provide substantial benefits in these aspects and are therefore an emerging technology in the hydraulic sector. ECD are displacement controlled cylinder drives with variable-speed pumps in a compact unit with an enclosed oil circuit. Alongside the advantage of improved ease-of-use compared to conventional hydraulic systems, ECD come with high robustness, high force capability and freely implementable fail-safe-behaviour compared to electro-mechanical screw drives (EMD). ECD are therefore primed to be a competitor to EMD, which have been replacing classical distributed hydraulic systems in many applications over the past years, mainly for modularisation reasons.

ECD with double-acting cylinders can generally be categorised in open hydrostatic circuit (OHC) and closed hydrostatic circuit (CHC). OHC refers to structures that connect one chamber of the cylinder to the baseline pressure of a reservoir or accumulator, while the other chamber is hydrostatically connected with one pump port. In order to create a system capable of operation in four quadrants of load, typically electric or hydraulic actuated valves are needed, see **Figure 1a**. CHC on the other hand means that both cylinder chambers are constrained with both pump ports, creating a closed kinematical chain, as depicted in **Figure 1b**. A requirement for CHC is a pump structure whose flow asymmetry matches the cylinder area ratio. Furthermore, suction valves are needed in order to define the minimum pressure in the circuit.
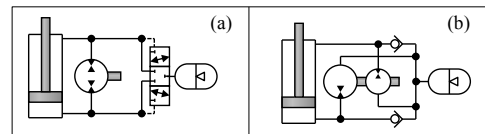

Figure 1: Exemplary circuitry structures for OHC with inverse shuttle valve (a) and CHC (b) drive solutions

In addition to the previously mentioned benefits of hydraulic cylinder drives compared to EMD, hydraulic circuits allow for variable transmission ratio by either varying effective pump displacement or effective cylinder area. This effect can be

conceived as variable pitch of a screw, if the analogy to electromechanical drives is sought [1]. In applications with a distinct separation between high load and rapid traverse strokes, such as hydraulic presses, variable transmission ratio enables downsizing of the electric drive. This effect is illustrated in **Figure 2** by means of single operation points: Assuming fixed transmission ratio, for speed stroke and force stroke the motor needs to be able to deliver both high rotational speed and high torque at different times of the cycle. If high force is only requested at low speed, by shifting to a higher transmission ratio the operation point of force stroke can be shifted towards high rotational speed and low torque. Thus, a motor with a lower specified torque can be used.
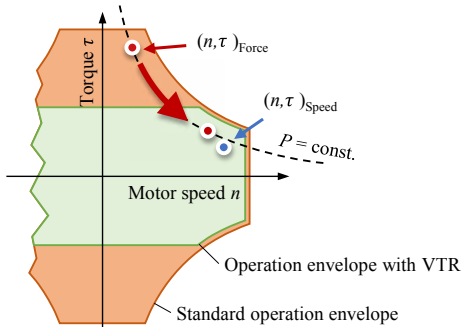

Figure 2: Illustration of motor downsizing through variable transmission ratio

It has previously been stated that in order to alter the transmission ratio, either variation of effective pump displacement (pump-based switching) or variation of effective cylinder area (actuator-based switching) can be applied. Pump-based switching can either be achieved by physically changing the displacement of a variable pump (continuous variation), or by combining multiple fixed displacement units by means of valves and manipulating output flow by activating or deactivating flows of single units (discrete variation). Actuator-based switching lacks the possibility of continuous variation of cylinder area for technological reasons, thus only variation of effective cylinder area by means of combination of different areas of a cylinder is possible (discrete variation). The resulting solution space of ECD with variable transmission ratio is described in **Table 1**. With reference to the system structure it can further be refined as to whether the individual transmission stages are implemented in OHC or CHC. Solutions with discrete pump-based

switching comprise a minimum of two pumps, solutions with discrete actuator-based switching at least to cylinder chambers.

The research project, which the paper at hand is based on, concentrated on ECD with at least one transmission stage in CHC using single rod cylinders. This configuration cannot be achieved with a single variable displacement pump, leading to neglecting continuously variable solutions.

Table 1: Solution space of ECD with two transmission stages

circuit type CHC/OHC	pump-based switching		actuator-based switching
	continuous	discrete	discrete
both stages OHC	PC0	PD0	AD0
one stage OHC/ one stage CHC	PC1	PD1	AD1
both stages CHC	PC2	PD2	AD2

Creating solutions with CHC structure in both transmission stages is a design problem within tight constraints concerning pump displacements and cylinder areas. A comprehensive approach to describe the subspace of these solutions is given by the authors for discrete pump-based switching [2] and discrete actuator-based switching [3], as well as state-of-the-art in switching linear drives.

Pioneer work on displacement controlled cylinder drives has been carried out by Sprockhoff [4] and Berbuer [5], dealing with OHC structures and valves to ensure a minimum pressure level in the cylinder and oil exchange with a reservoir. Important foundations for asymmetric single rod cylinders with displacement control in CHC structure have been laid by Lodewyks [5]. More recent research by Michel examined both OHC and CHC types, proving that OHC tend to be more energy efficient, while CHC having the better controllability [6, 7]. It has been shown that OHC structures with inverse shuttle valves exhibit discontinuities and instabilities when the load pressure is around zero or changes directions. Instability issues through pressure-piloted switching valves in this context have been investigated in further research [8, 9]. A good overview over the current state of the art in ECD is included in the work by Ketelsen et al. [10].

2. DOWNSIZING POTENTIAL

2.1. Dimensioning of electric drivetrain

Choice of electric motors and servo inverters are crucial to ECD drives, since they are strongly related with their static and dynamic properties as well as total costs. In the following, dimensioning is carried out with relation to typical combinations of servo inverters and synchronous servo motors.

Usually, servo motors are dimensioned so that they withstand the thermal load over a specific cycle and the maximum dynamic torque that occurs over time. The **maximum torque criterion (MTC)** can be formulated as the following:

$$\max\big(\tau(t)\big) < \tau_{M,max} \tag{1}$$

As a thermal criterion, a motor exhibits an S1-line $\tau_{M1}(n)$ in the torque-speed plane, which has to lie towards the outside of operating point of equivalent load (n_{eq}, τ_{eq}) of the motor during its load cycle. It is often an acceptable simplification to assume the S1-curve to be parallel to the speed axis, thus for generalisation purposes this will apply. The torque value of the horizontal S1-line will be referred to as the nominal torque τ_N. Thus, the thermal criterion (**equivalent torque criterion, ETC**) reads

$$\tau_{eq} < \tau_{M,nom} \tag{2}$$

with the equivalent torque

$$\tau_{eq} = \sqrt{\frac{1}{T} \int_T \tau(t)^2 \ dt}. \tag{3}$$

This equivalent torque formulation correlates the electric losses of the motor to the square of the torque according to the following:

$$P_{loss}(t) \propto I(t)^2 \propto \tau(t)^2 \tag{4}$$

Any electric motor has to fulfil both maximum torque and equivalent torque criterion that are calculated based on the torque regime $\tau(t)$ of the load cycle.

2.2. Choice of transmission ratios

ECD can be regarded as transmission that transform rotational mechanical input power into translational mechanical output power. The transmission ratio can be defined as

$$i = \frac{\omega}{\dot{x}} = \frac{2\pi n}{\dot{x}} \tag{5}$$

Neglecting losses, conservation of energy results in

$$i = \frac{F}{\tau}. \tag{6}$$

For the simplified and idealised ECD structure shown in **Figure 3**, the transmission ratio yields

$$i = \frac{2\pi \, A_{eff}}{V_{P,eff}}. \tag{7}$$
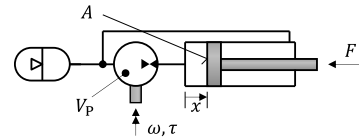

Figure 3: Simplified structure of ECD

It is obvious that, by changing effective cylinder area A_{eff} or effective pump displacement volume $V_{P,eff}$, the transmission ratio can be varied.

Let i^F be the transmission ratio in force stage, and i^S the transmission ratio in speed stage of any drive with variable transmission ratio. The transmission range is defined as

$$\alpha_i = \frac{i^F}{i^S} \tag{8}$$

and from eqs. (5)-(6) we can derive

$$\alpha_i = \frac{\tau^S(F)}{\tau^F(F)} = \frac{n^F(\dot{x})}{n^S(\dot{x})}. \tag{9}$$

For calculation of downsizing potential, following hypothesis is used:

The size of an electric servo drive is minimal if the required torque is minimal.

Thus, a drive dimensioning minimises the drive size, whenever it maximises the rotational speed. In direct-driven hydraulics, pumps are typically the limiting factor of rotational speed, thus the goal is to reach the maximum pump speed in both force and speed stage:

$$\big|n^S\big|_{max} = \big|n^F\big|_{max} = n_{max} \tag{10}$$

Neglecting leakage, the rotational speed is

$$n(t) = \begin{cases} \dfrac{i^S}{2\pi} \cdot \dot{x}(t) \text{ , in speed stage} \\ \dfrac{i^F}{2\pi} \cdot \dot{x}(t) \text{ , in force stage.} \end{cases} \tag{11}$$

Thus, an optimal transmission range can be derived as the ratio of maximum speed in speed stage over maximum speed in force stage:

$$\alpha_i = \frac{\big|\dot{x}^S\big|_{max}}{\big|\dot{x}^F\big|_{max}} \tag{12}$$

Neglecting friction losses, the torque yields

$$
\tau(t) = \begin{cases} \dfrac{F(t)}{i^{S}} & \text{, in speed stage} \\ \dfrac{F(t)}{i^{F}} & \text{, in force stage.} \end{cases} \tag{13}
$$

2.3. Downsizing potential for electric motors

For a reference, an ECD with fixed transmission ratio is dimensioned in a way that it reaches the maximum pump speed. The equivalent torque is

$$
\tau_{eq,Ref} = \sqrt{\frac{1}{T_{tot}} \int_{T_{tot}} \left(\frac{F(t)}{i_{Ref}} \right)^2 \, dt} \tag{14}
$$

while maximum torque yields

$$
\tau_{max,Ref} = \frac{F_{max}}{i_{Ref}}. \tag{15}
$$

The load cycle is divided in a speed stage T_S and a force stage T_F, see **Figure 4**, and the transmission of the switching drive is chosen accordingly.
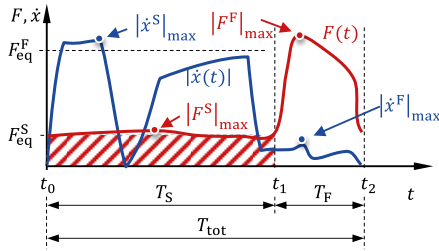

Figure 4: Exemplary machine cycle

According to the findings in eq. (12) and an optimally dimensioned reference transmission ratio, following transmission ratios can be assumed:

$$
i_{Ref} = i^{S} = \frac{i^{F}}{\alpha_i} \tag{16}
$$

With this definition, we can calculate the ratio between the equivalent torque of the reference drive over the equivalent torque of the switching drive $\alpha_{\tau,eq}$:
    After introducing proportional parameters

$$
\alpha_F = \frac{F_{eq}^{F}}{F_{eq}^{S}} \tag{17}
$$

$$
\alpha_t = \frac{T_F}{T_S} \tag{18}
$$

and with definition of an equivalent force

$$
F_{eq} = \sqrt{\frac{1}{T} \int_{T} F(t)^2 \, dt} \tag{19}
$$

the equivalent torque ratio results in

$$
\alpha_{\tau,eq} = \frac{\tau_{eq}}{\tau_{eq,Ref}} = \sqrt{\frac{1 + \dfrac{\alpha_F^2 \cdot \alpha_t}{\alpha_i^2}}{1 + \alpha_F^2 \cdot \alpha_t}}. \tag{20}
$$

The ratio of maximum torques is

$$
\alpha_{\tau,max} = \frac{\tau_{max}}{\tau_{max,Ref}} = \min\left(\alpha_i, \frac{|M^{E}|_{max}}{|M^{K}|_{max}} \right). \tag{21}
$$

With these parameters $\alpha_{\tau,eq}$, $\alpha_{\tau,max}$ an assessment of downsizing potential can be made. If both reference fixed drive and variable transmission drive are limited by the equivalent torque criterion, the downsizing parameter concerning rated torque is equal to the equivalent torque ratio $\alpha_{\tau,eq}$. However, this is not always the case, thus differentiation has to be made.

Whether a motor is limited by maximum torque or equivalent torque depends on its overload capacity, meaning the ratio of maximum torque to nominal torque:

$$
\alpha_{OL} = \frac{\tau_{Mot,max}}{\tau_{Mot,nom}} \tag{22}
$$

For generalisation, we assume that all feasible motors that are within the choice range share the same overload capacity α_{OL}. Under this circumstance, downsizing factors with respect to torque specifications are listed in **Table 2**. The downsizing factor means the ratio of reduction of required nominal motor torque that can be achieved by means of transmission switching against a fixed transmission reference drive:

$$
\alpha_{\tau,Mot} = \frac{\tau_{M,nom}}{\tau_{M,nom,Ref}} \tag{23}
$$

The resulting calculation schedule for downsizing potential is thus:

1. Choose force stage intervals and speed stage intervals according to the load cycle.
2. Calculate transmission range with eq. (12) and $\alpha_{\tau,eq}$ using eqs. (17)-(20).
3. Choose a realistic overload capacity α_{OL}
4. Select case and calculate downsizing factor $\alpha_{\tau,Mot}$ according to Table 2.

Table 2: Calculation of downsizing factors depending on load conditions

	Limiting criteria	Condition	Downsizing factor
Case 1	Reference → MTC Switching drive → MTC	$\dfrac{F_{max}}{\alpha_i \cdot F_{eff} \cdot \alpha_{\tau,eq}} > \alpha_{OL}$	$\alpha_{\tau,Mot} = \alpha_{\tau,max}$
Case 2	Reference → MTC Switching drive → ETC	$\dfrac{F_{max}}{F_{eff}} > \alpha_{OL} > \dfrac{F_{max}}{\alpha_i \cdot F_{eff} \cdot \alpha_{\tau,eq}}$	$\alpha_{\tau,Mot} = \dfrac{\alpha_{OL} \cdot F_{eff} \cdot \alpha_{\tau,eq}}{F_{max}}$
Case 3	Reference → ETC Switching drive → ETC	$\alpha_{OL} > \dfrac{F_{max}}{F_{eff}}$	$\alpha_{\tau,Mot} = \alpha_{\tau,eq}$

Switching transmission ratio also has an effect on the choice of servo inverters. These are often dimensioned to withstand the maximum current during the cycle, which correlates with maximum torque. Thus, the downsizing factor can be considered to be

$$\alpha_{I,Inv} = \alpha_{\tau,max} \tag{24}$$

This methodology is applied to an idealised cycle of a hydraulic press brake in the following. The cycle data is given in **Figure 5** (left) by means of cylinder position and speed as well as load force curves over time. The resulting motor torque and speed are shown in the diagram in the middle of the same figure, for a reference drive with fixed transmission and an ECD with variable transmission. Switching is carried out at the times

t_a and t_b. By evaluating the cycle in the described manner, the downsizing factor of the motor results in $\alpha_{\tau,Mot} = 0.22$ (case 3) and $\alpha_{I,Inv} = 0.19$ for the inverter. Using an exemplary model range of synchronous servo motors and inverters in the power range of 1 to 10 kW, the benefits of variable transmission in terms of weight and cost savings are given in Figure 5 on the right.

3. DEMONSTRATOR DRIVES

In order to validate the findings from the project, two demonstrator ECD that arose from the systematic scan of solution space [3, 2] have been set up – one for each switching principle – as depicted in **Figure 6**.

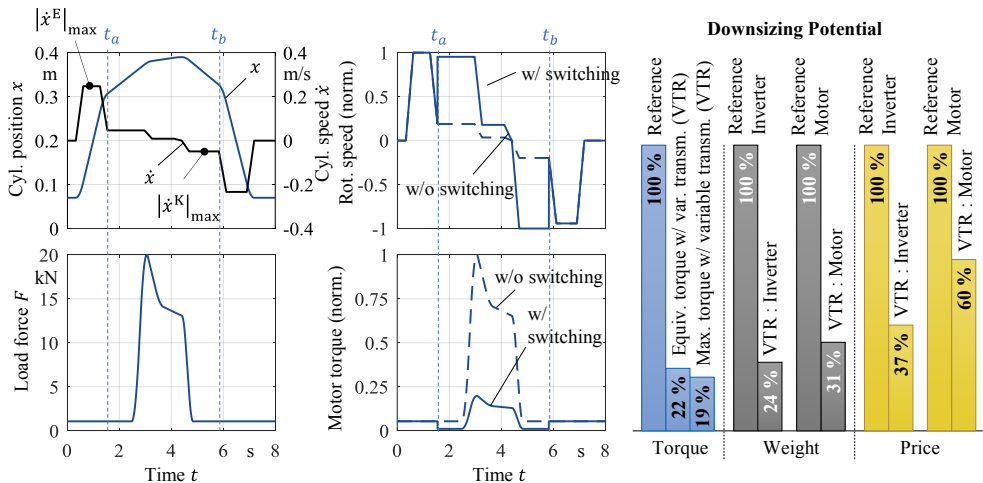The pump-based switching demonstrator (PBD) makes use of a CHC structure in speed

Figure 5: Cycle of an idealised press brake with motor torque and speed with and without switching transmission, and downsizing in terms of weight and cost of exemplary commercially available component.
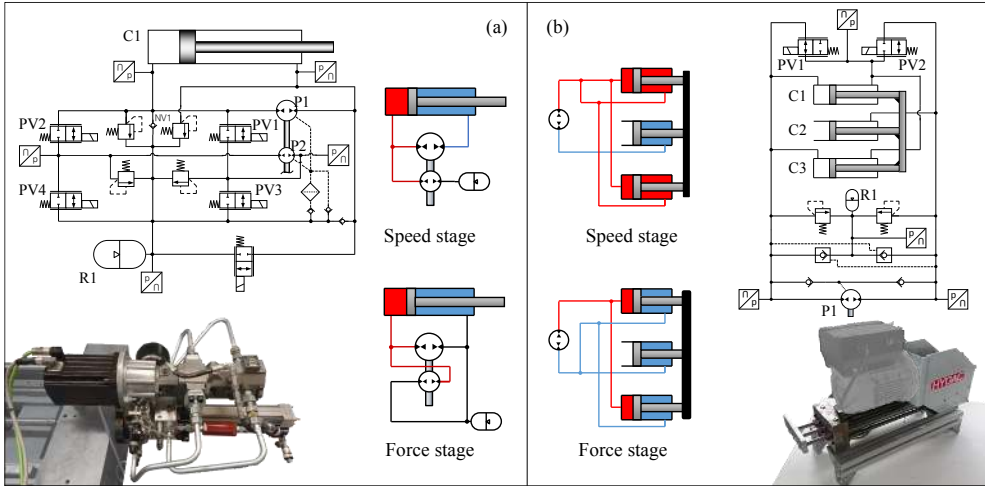
Figure 6:   Demonstrators PBD (a) and ABD (b)

stage, where the sum of two pump outflows is connected to the head-side cylinder chamber while the rod-side chamber receives the flow only from the larger pump. Due to CHC, the ratio of pump displacement volumes has to be related to the cylinder area ratio. In force stage, an OHC is applied such, that the rod-side chamber is connected with the reservoir. The head side chamber receives a flow that results from the difference of both pump outflows. Torque reduction is due to one unit working in pump mode, and the other working in motoring mode on the same shaft. Switching is carried out via five 2/2 directional proportional solenoid cartridge valves. For details see [2].

The actuator-based switching demonstrator (ABD) comprises three parallel, identical single rod cylinders with mechanically coupled piston rods. In force stage, one pump port acts on the three rod-side chambers, while the other pump port acts on the two outer head-side chambers. The centre head-side chamber is constantly vented. In speed stage, the two outer rod side chambers are switched to the other pump port. Since the cylinders are dimensioned in a way that the cylinder unit acts as a statically symmetrical consumer in both stages, it can be operated in CHC with a single pump. However, in order to avoid any undesired pressure increase, pilot operated check valves are used to define the minimum pressure in the used system. Switching valves are two valves identical to the ones used in PBD. More details on this demonstrator can be found in [3].

In terms of the systemisation shown in Table 1, PBD can be considered PC1 and ABD can be considered AD2.

Significant parameters for both systems are listed in **Table 3**.

Table 3:   Demonstrator dimensioning parameters

	PBD	ABD
Pump displacement	$V_{P1} = 10{,}8 \text{ cm}^3$ $V_{P2} = 6{,}9 \text{ cm}^3$	$V_{P1} = 5 \text{ cm}^3$
Cylinder dimensions	ø(40mm/25mm) x 450 mm	ø(25mm/14,43mm) x 400 mm
Reservoir	$V_{tot} = 1{,}4\,\text{l}$	$V_{tot} = 80$ ml
transm. range	1 : 4.5	1 : 3

4. SWITCHING STRATEGY

The aim of the switching process is to change the transmission. Obviously, a discontinuous switch to a different transmission ratio will lead to a disturbance of the system, similar to a step in the primary command signal of the prime mover.

In order to allow a smooth transition, valve trajectories are generated such that the transmission ratio is a smooth curve from start to end of the process. Further we demand

$$i^F \geq \frac{\omega(t)}{\dot{x}(t)} \geq i^S \tag{25}$$

throughout the switching process. Since due to valve opening, the drive is no longer a hydrostatic transmission, the load has to be taken into account.

4.1. Systematisation

In previous work [3, 2], the definition of a transmission stage allocates each pump port to any cylinder port or the reservoir port in case of pump-based switching, or allocates each cylinder port to any pump port or the reservoir in case of actuator-based switching, respectively. Thus, any switching process can be thought of as a sequence of reallocations of pump ports (pump-based switching) or cylinder ports (actuator-based switching). Reallocation of one port is called an elementary switching process (ESP), which is illustrated in **Figure 7**.
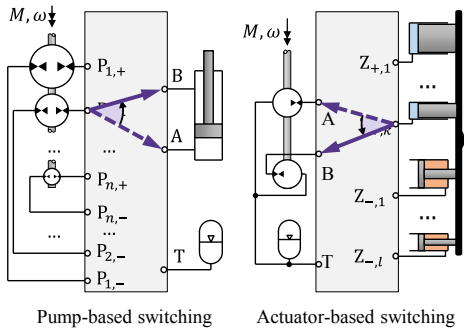

Figure 7: Examples of elementary switching processes

Any such ESP, of which global switching processes are constituted, have the logic of an electric two-way switch, or a 3/2-directional valve. A general way of realisation with one more degree of freedom is a combination of two 2/2-directional valve per ESP, as shown in **Figure 8**.
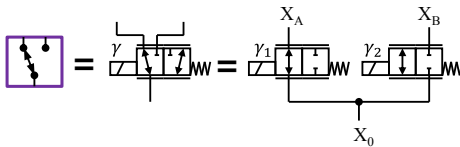

Figure 8: Valve architectures for ESP

The advantage of separating the switching process in ESP is unification of control strategies. Since all ESP can be treated similarly, even complex global switching processes can be broken down to manageable units.

The meaning of ESP in terms of the demonstrator drives is given in **Figure 9**. For PBD, there are two ESP that have to be switched consecutively. Between the two ESP, there is an intermediate state, in which the smaller pump idles at negligible pressure difference. The exact order, in which ESP1 and ESP2 are switched decide on

whether the pump idles at the pressure level of the reservoir or of the cylinder's head-side chamber. Before any switching is carried out, PV5 has to be opened in order to open the hydrostatic circuit on the rod-side chamber to reservoir. In case of ABD, only one ESP is required.
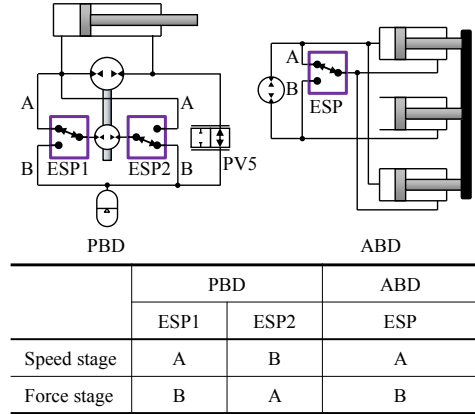

	PBD		ABD
	ESP1	ESP2	ESP
Speed stage	A	B	A
Force stage	B	A	B

Figure 9: ESP in demonstrator drives and state table

With reference to the nomenclature in **Figure 6**, ESP1 of PBD consists of valves PV2 and PV4, while ESP2 consists of PV1 and PV3. As to ABD, ESP obviously consists of PV1 and PV2.

4.2. Elementary switching process

Although all ESP have the same structure, the boundary conditions do vary between pump-based and actuator-based switching. With reference to the port labels in **Figure 8**, pump-based ESP can be considered to have an independent flow input at port X_0 due to exclusively having one pump port directly attached, and independent pressure input at port X_A and X_B depending on load. When considering actuator-based switching, flows and pressure on all ports depend on interaction of loads, pump speeds and valve positions. However, strategies developed for the simpler pump-based switching proved to work for actuator-based switching as well.

Modelling of ESP is carried out based on the system depicted in **Figure 11**. It is governed by turbulent valve flow and flow continuity:

$$Q_0 = Q_A + Q_B \tag{26}$$

$$Q_A = B \cdot \gamma_A \cdot \text{sgn}(p_0 - p_A) \cdot \sqrt{|p_0 - p_A|} \tag{27}$$

$$Q_B = B \cdot \gamma_B \cdot \text{sgn}(p_0 - p_B) \cdot \sqrt{|p_0 - p_B|} \tag{28}$$

B is the turbulent flow coefficient that accounts for nominal valve flow at a given pressure difference.
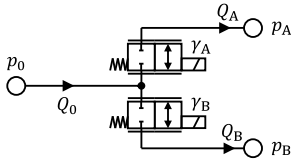

Figure 11: ESP model

Control strategies for the proportional valves of an ESP are based on a static analysis of the switching process with the boundary conditions of pump-based switching at constant motor speed and constant load. An exemplary analysis under such constraints is given in **Figure 10** in the plane over the two normalized openings of the valves involved. Any switching process requires a transition from point X to Y or vice versa across the plane. Any trajectory through the plane results in increased loss over the valve control edges. Every load and speed condition exhibits a saddle point of minimum unavoidable power loss, marked with 'M' in the given example.

Choosing a bilinear valve trajectory through the saddle point 'M' as shown in Figure 10 minimises losses and fulfils eq. (25). Moving the corner point further towards the upper right results in flow losses (short-circuit flow across the valves ($Q_A < 0$)) and thus violates eq. (25). Moving it further down towards lower γ_B results in drastic pressure increase and thus torque loss. At negative Q_0 it would even lead to serious cavitation.

With such valve trajectories, the challenge is to meet accuracy requirements using simple direct solenoid driven valves without spool position feedback. Around point 'M' the pressure p_0 is sensitive to valve spool position, leading to dynamic excitation of the system especially at actuator-based switching.

A more robust strategy therefore makes use of a p_0 pressure feedback to 'guide' one valve control signal along it correct trajectory. An overview of the strategy is given in the following, with reference to Figure 10:

Depending on flow direction of Q_0 and direction of pressure difference across the switch $p_A - p_B$, the saddle point 'M' lies on one of the axes γ_A or γ_B. As a characteristic property of the proposed control strategy, the valve command signal on whose axis 'M' is located, is governed by a pressure feedback controller. In the example given in Figure 10, this is signal γ_B. For the exemplary transition from point X to point Y, the control strategy is given in **Figure 12** by means of state chart notation.
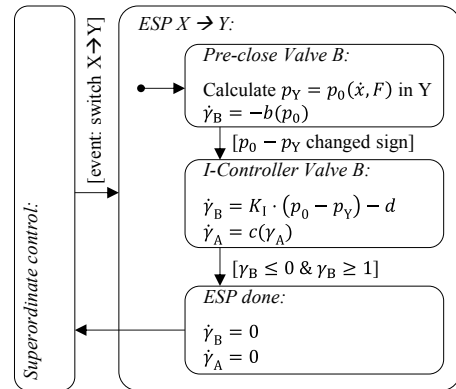

Figure 12: ESP sequence X→Y, see Figure 10

First, the valve B is closed using a trajectory that takes p_0 into account in order to prevent overshoot. During that process, the pressure p_0 corresponding to point 'Y' is constantly calculated based on measurement data. Once p_0 reaches that
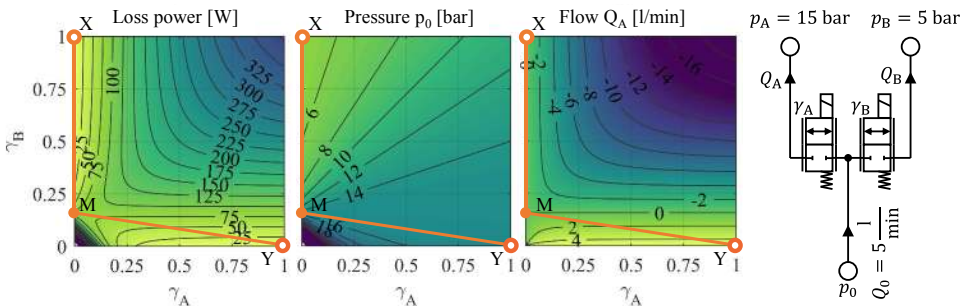

Figure 10: Static behaviour of the ESP for exemplary boundary conditions

pressure p_Y, the integral pressure feedback controller is activated to keep p_0 at p_Y while opening valve A. The term d in the pressure feedback control law makes sure that valve B closes and the switching process carries on. When the conditions of point 'Y' are met in terms of valve command signals, the ESP is completed. The parameters or functions K_I, b, c, d have an impact on the smoothness and duration of the ESP, however an optimal set is yet to be defined and depend strongly on the dynamic properties of the system and valves.

5. VALIDATION

The pump-based switching demonstrator is used to validate both the switching strategy and the downsizing potential on a load test stand. In the following, a range of experimental results will be presented. Results using ABD remain subject of future publications.

5.1. Switching strategy

The first example shown is a switching procedure from speed stage to force stage at constant motor speed of $n = 1000 \text{ min}^{-1}$ for different load forces, with result plotted in **Figure 13**. The cylinder velocity at low load force ($F = 1 \text{ kN}$) took a smooth decline over the course of switching, regardless of whether the smooth switching strategy was applied ($\Delta t = 0.25 \text{ s}$) or whether all valves were operated at the same time and as fast as possible ($\Delta t = 0 \text{ s}$). The smooth transition at discrete switching operation may be due to low response of the valve, but cannot be verified since spool position measurement is not implemented.
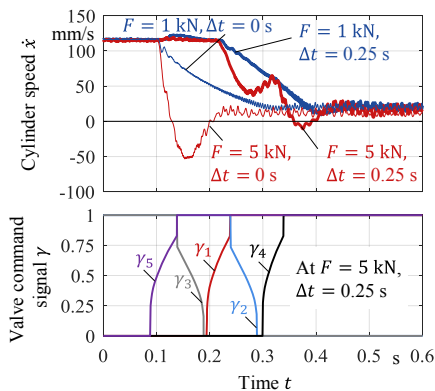

Figure 13: Switching from speed stage to force stage at $n = 1000 \text{ min}^{-1}$ at constant load force F

At higher load, the smooth switching strategy yields a smoother transition and less overshoot than discrete switching. When all valves are actuated at one time, uncontrolled short-circuit flow makes the mass accelerate in direction of external load, which is prevented using the above described valve trajectory.

The bottom diagram of Figure 13 shows the valve command signals during the controlled switching process. Integral-dominated pressure feedback control lets both valves be closed at the same times ($t = 0.19 \text{ s}$ and $t = 0.29 \text{ s}$) in both ESP. That would mean the flow to be blocked and dramatic pressure increase or cavitation at on pump port. The absence of these proves that the spool positions of the closing valves lack behind their command signal significantly.

A similar switching procedure was run at a motor speed that was generated by a dynamic feedforward control to keep the cylinder speed constant. The controller calculates the motor speed according to desired cylinder speed trajectories, taking plant dynamics, load force and valve positions into account. Measurement result are shown in **Figure 14**.
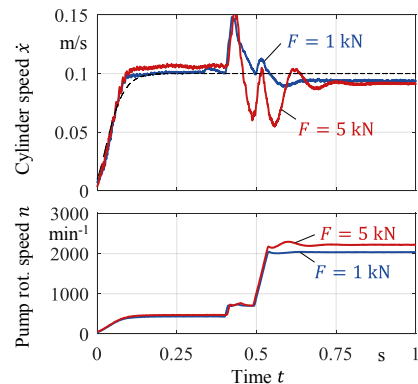

Figure 14: Switching from speed stage to force stage at constant load force F and with feedforward speed control

It becomes obvious that while switching, the trajectory cannot be tracked by the motor speed command. The reason is mainly related to deviations between valve command signal and actual spool opening. The feedforward control law receives the valve command signal and calculates required rotational speeds based on these.

5.2. Downsizing potential

Downsizing potential of the demonstrator drive

can be assessed by mapping the torque require-
ment over speed and load force in speed stage and
force stage. The associated measurement results
are illustrated in **Figure 15**. Speed stage record-
ings could not exceed a load force of 7 kN in the
experiment, since the used motor was restricted
to a nominal torque of 20 Nm. Linear extrapola-
tion of the curves however is admissible. A
torque reduction due to force stage can clearly be
observed at high load force. Given a maximum
torque of 20 Nm, the achievable force in force
stage is about three times the achievable force in
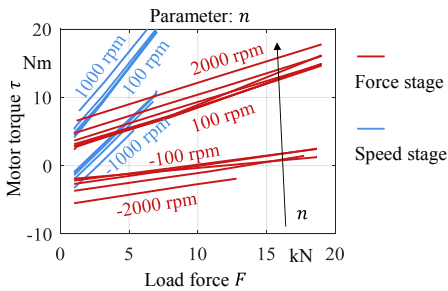speed stage.

Figure 15: Measurement of torque over speed and force

As further proof of concept, the press brake cycle
analysed in Figure 4 is implemented on the load
test bench. The results in terms of torque are com-
pared in **Figure 16** for the demonstrator in speed
stage only and with switching activated. The re-
sulting ratios of maximum and equivalent force
are $\alpha_{\tau,\max} = 0.31$ and $\alpha_{\tau,\max} = 0.43$ respec-
tively, resulting in the estimated cost reduction
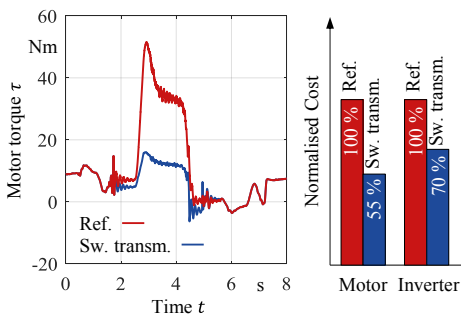shown in Figure 16.

Figure 16: Measurement of torque in press brake cycle
from Figure 5, for reference and switching
driving

The cost reduction is lower compared to the re-
ductions estimated under ideal conditions, as
shown in Figure 5. This is mainly due to to

causes: Firstly, pump friction has a major impact
on motor torque in force stage and, secondly, the
transmission range of the demonstrator is lower
than the optimal transmission range for the cho-
sen load cycle, due to a restricted choice of cylin-
der area ratios, as documented in [2].

6. CONCLUSION AND OUTLOOK

The paper at hand provides a guideline on how to
estimate the downsizing potential of variable
transmission linear drives in comparison to fixed
transmission drives, depending on a given load
cycle. For an exemplary press brake cycle, the
maximum downsizing potential is estimated to be
around 80 % in terms of torque. Using a demon-
strator drive, the achievable downsizing potential
was reduced to 57 % mainly due to pump friction.
Even with friction related losses, substantial cost
savings of the electric components can be real-
ised.

A general approach to handle switching pro-
cesses for discrete variable transmission drives is
given and applied to the demonstrators. Switch-
ing smoothness was found to be improved with
valve trajectories based on pressure feedback in
comparison to discrete switching, although valve
accuracy proved to be crucial to attainable
switching smoothness in general. When it comes
to adoption of the strategy for application in pro-
duction machinery, thorough measurement and
characterization of the used valves is necessary to
meet accuracy specifications when switching un-
der load occurs.

Approaches that may be investigated in future
work are ballistic switching strategies that might
be applied when inertia is high in comparison to
external load forces.

ACKNOWLEDGEMENT

NOMENCLATURE

ABD   Actuator-based switching demonstrator

CHC   Closed hydrostatic circuit

ECD	Electro-hydrostatic compact drive
EMD	Electromechanical drive
ESP	Elementary switching process
ETC	Equivalent torque criterion
MTC	Maximum torque criterion
OHC	Open hydrostatic circuit
PBD	Pump-based switching demonstrator
VTR	Variable transmission ratio
eff	Effective
eq	Equivalent
F	Force stage
max	Maximum
Mot	Motor
nom	Nominal
OL	Overload
P	Pump ports
Inv	Inverter
Ref	Reference
S	Speed stage
T	Reservoir port
tot	Total
X	Port label
X,Y	Operation points
Z	Cylinder ports

A	Area	m²
B	Flow coefficient	$m^3/s\sqrt{Pa}$
b	control parameter	1/s
c	control function	1/s
d	control parameter	1/s
F	Force	N
I	Electric current	A
i	Transmission ratio	-
K_I	Integral gain	1/Pa s
n	Rotational speed	1/s
p	Pressure	Pa
P	Power	W
Q	Flow rate	m³/s
t	Time	s
T	Time interval	s
V_P	Pump displacement volume	m³
x	Cylinder position	m

α	Ratio parameter	-
γ	Normalised valve command signal	-
τ	Torque	Nm
ω	Angular speed	rad/s

REFERENCES

[1] Brahmer, B.: On Adaptive Electro Hydrostatic Actuators. In: *Proceedings of the 11th International Fluid Power Conference (11. IFK)*. Aachen, Germany, 2018

[2] Kolks, G.; Weber, J.: Compact Cylinder Drives with Variable Transmission Ratio Using Multiple Pumps. In: *Proceedings of the 10th Workshop on Digital Fluid Power*. Linz, AT, 2019

[3] Kolks, G.; Weber, J.: Symmetric Single Rod Cylinders with Variable Piston Area? A Comprehensive Approach to the Right Solution. In: *Proceedings of the ASME/BATH 2018 Symposium on Fluid Power & Motion Control* : *FPMC 2018*. Bath, UK, 2018

[4] Sprockhoff, V.: *Untersuchungen von Regelungen im hydrostatischen Zylinderantrieb mit Servopumpe*. RWTH Aachen. Dissertation. 1979

[5] Berbuer, J.: *Neuartige Servoantriebe mit primärer Verdrängersteuerung*. RWTH Aachen. Dissertation. 1988

[6] Michel, S.; Weber, J.: Electrohydraulic compact-drives for low power applications. In: *Proceedings of the 7th FPNI PhD-Symposium on Fluid Power*. Reggio Emilia, Italy, 2012

[7] Michel, S.: *Energieeffiziente elektrohydraulische Antriebe kleiner Leistung*. Dresden, TU Dresden. Research Report. 2012

[8] Çalışkan, Hakan; Balkan, Tuna; Platin, Bülent E.: *A Complete Analysis and a Novel Solution for Instability in Pump Controlled Asymmetric Actuators*. In: *Journal of Dynamic Systems, Measurement, and Control* 137 (2015), Nr. 9, 091008-091008-14

[9] Williamson, C.; Ivantysynova, M.: Stability and motion control of inertial loads with displacement controlled hydaulic actuators. In: *Proceedings of the 6th FPNI PhD-Symposium on Fluid Power*. West Lafayette, USA, 2010

[10] Ketelsen, Søren; Padovani, Damiano; Andersen, Torben; Ebbesen, Morten; Schmidt, Lasse: *Classification and Review of Pump-Controlled Differential Cylinder Drives*. In: *Energies* 12 (2019), Nr. 7, p. 1293